Stereodynamics of 9,11-Diphenyl-10-azatetracyclo[6.3.0.0.^{4,11}0.^{5,9}]undecanes. Highly Restricted Nitrogen Inversion and Isolated Phenyl Rotation. X-ray Crystallographic, Dynamic NMR, and Molecular Mechanics Studies

Gordon W. Gribble,* Frank L. Switzer, and John H. Bushweller

Department of Chemistry, Dartmouth College, Hanover, New Hampshire 03755-3564

John G. Jewett, Jay H. Brown, Jessica L. Dion, and C. Hackett Bushweller*

Department of Chemistry, University of Vermont, Burlington, Vermont 05405-0125

Marianne P. Byrn* and Charles E. Strouse

Department of Chemistry and Biochemistry, The J. D. McCullough X-ray Crystallography Laboratory, University of California, Los Angeles, California 90095-1569

Received December 8, 1995[⊗]

The ^{1}H NMR spectra of 10-benzyl-9,11-diphenyl-10-azatetracyclo[6.3.0.0.^{4,11}0.^{5,9}]undecane (**BnPh$_2$**) and 10-methyl-9,11-diphenyl-10-azatetracyclo[6.3.0.0.^{4,11}0.^{5,9}]undecane (**MePh$_2$**) decoalesce due to slowing inversion at nitrogen and to slowing isolated bridgehead phenyl rotation. The high nitrogen inversion barriers in **MePh$_2$** ($\Delta G^‡ = 12.2 \pm 0.1$ kcal/mol at 250 K) and **BnPh$_2$** ($\Delta G^‡ = 10.6 \pm 0.1$ kcal/mol at 215 K) are typical of tertiary amines in which at least one C−N−C bond angle is constrained to a small value. Compared to the minuscule rotation barriers about sp^2−sp^3 carbon−carbon bonds in simple molecular systems, the bridgehead phenyl rotation barriers in **MePh$_2$** ($\Delta G^‡ = 9.8 \pm 0.1$ kcal/mol at 210 K) and **BnPh$_2$** ($\Delta G^‡ = 9.8 \pm 0.1$ kcal/mol at 210 K) are unusually high. Molecular mechanics calculations (MMX force field) suggest that the origin of the high phenyl rotation barriers lies in the close passage of an *o*-phenyl proton and a methyl (or benzylmethylene) proton in the transition state. **BnPh$_2$** crystallized from hexane as white needles in the monoclinic system *Pn*. Unit cell dimensions are as follows: $a = 12.198(1)$ Å, $b = 6.1399(6)$ Å, $c = 14.938(2)$ Å, $\beta = 107.470(4)°$, $V = 1067.1(2)$ Å^3, $Z = 2$. In the crystal molecular structure, the imine bridge CNC bond angle in **BnPh$_2$** is constrained to a small value (96°). The benzylic phenyl group is oriented gauche to the nitrogen lone pair.

Introduction

Since early unsuccessful attempts to resolve simple chiral amines suggested facile inversion at the pyramidal nitrogen, extensive experimental and computational studies have provided significant insight into the sometimes complex internal motions associated with nitrogen inversion in tertiary amines.[1,2] It is now well established that constraining one central CNC bond angle of a tertiary amine to a small value by incorporation into a small ring or into a rigid bicyclic framework induces high barriers to nitrogen inversion.[2−8] It is most likely that the high barriers are due to angle strain in the quasi-trigonal planar transition state,[4] although the argument has been advanced that, in these bicyclic systems, delocalization of the nitrogen lone pair into the bicyclic framework leads to special ground state stabilization.[8]

Another important and prevalent internal molecular motion is rotation about sp^2−sp^3 carbon−carbon bonds.[9,10] In simple systems such as toluene and *tert*-butylbenzene, the barriers to 6-fold methyl and *tert*-butyl rotation are minuscule (0.14, 0.6 kcal/mol).[11,12] In more highly substituted systems that are more sterically crowded, barriers can range from 8 to 45 kcal/mol.[9,13−15] In a similar fashion, buttressing of the phenyl group in di-*tert*-butylphenylphosphine leads to a phenyl rotation barrier equal to 10.5 kcal/mol.[16]

As part of our continuing studies of restricted nitrogen inversion in the 7-azabicyclo[2.2.1]heptyl ring system[4,17,18] including efforts to assess the nature of the "bicyclic

⊗ Abstract published in *Advance ACS Abstracts,* June 1, 1996.

(1) For a recent review, see: Bushweller, C. H. In *Acyclic Organonitrogen Stereodynamics*; Lambert, J. B., Takeuchi, Y., Eds.; VCH Publishers: New York, 1992.
(2) For previous reviews, see: Rauk, A.; Allen, L. C.; Mislow, K. *Angew. Chem., Int. Ed. Engl.* **1970**, *9*, 400. Lehn, J. M. *Fortschr. Chem. Forsch.* **1970**, *15*, 311. Lambert, J. B. *Top. Stereochem.* **1971**, *6*, 19.
(3) Nelsen, S. F.; Ippoliti, J. T.; Frigo, T. B.; Petillo, P. A. *J. Am. Chem. Soc.* **1989**, *111*, 1776.
(4) Bushweller, C. H.; Brown, J. H.; DiMeglio, C. M.; Gribble, G. W.; Eaton, J. T.; LeHoullier, C. S.; Olson, E. R. *J. Org. Chem.* **1995**, *60*, 268 and references therein.
(5) Davies, J. W.; Malpass, J. R.; Fawcett, J.; Prouse, L. J. S.; Lindsay, R.; Russell, D. R. *J. Chem. Soc., Chem. Commun.* **1986**, 1135.
(6) Davies, J. W.; Durrant, M. L.; Walker, M. P.; Belkacemi, D.; Malpass, J. R. *Tetrahedron* **1992**, *48*, 861.
(7) Davies, J. W.; Durrant, M. L.; Walker, M. P.; Malpass, J. R. *Tetrahedron* **1992**, *48*, 4379.
(8) Belkacemi, D.; Davies, J. W.; Malpass, J. R.; Naylor, A.; Smith, C. R. *Tetrahedron* **1992**, *48*, 10161.
(9) Oki, M. *Applications of Dynamic NMR Spectroscopy to Organic Chemistry*; VCH Publishers: Deerfield Beach, 1985.
(10) Orville-Thomas, W. J., Ed. *Internal Rotation In Molecules*; J. Wiley and Sons: New York, 1974.
(11) Rudolph, H. D.; Dreizler, H.; Jaeschke, A.; Wendling, P. *Z. Naturforsch.* **1967**, *22A*, 940.
(12) Campanelli, A. R.; Ramando, F.; Domenicano, A.; Hargittai, I. *J. Phys. Chem.* **1994**, *98*, 11046.
(13) Gribble, G. W.; Olson, E. R.; Brown, J. H.; Bushweller. C. H. *J. Org. Chem.* **1993**, *58*, 1631.
(14) Lomas, J. S.; Anderson, J. E. *J. Org. Chem.* **1995**, *60*, 3246.
(15) Garcia, R.; Riera, J.; Carilla, J.; Julia, L.; Sanchez-Baeza, F. J.; Molins, E. *Tetrahedron* **1995**, *51*, 3627.
(16) Rithner, C. D.; Bushweller, C. H. *J. Am. Chem. Soc.* **1985**, *107*, 7823.

S0022-3263(95)02185-2 CCC: $12.00

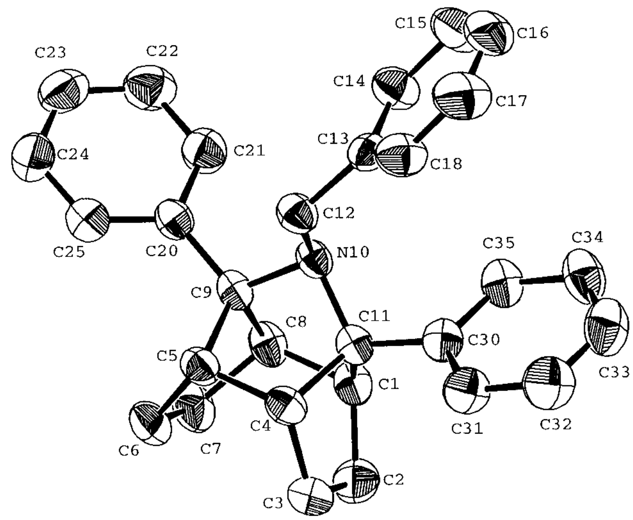

Figure 1. ORTEP view of the molecular structure in crystalline **BnPh₂** including the atom labeling scheme. The hydrogens have been omitted for clarity. Thermal ellipsoids are drawn at the 50% probability level.

effect" on nitrogen inversion,[2,8] we pursued detailed studies of the stereodynamics of 10-benzyl-9,11-diphenyl-10-azatetracyclo[6.3.0.0.^{4,11}0.^{5,9}]undecane (**BnPh$_2$**) and 10-methyl-9,11-diphenyl-10-azatetracyclo[6.3.0.0.^{4,11}0.^{5,9}]-undecane (**MePh$_2$**). This paper reports the X-ray crystallographic structure of **BnPh$_2$** and dynamic NMR (DNMR) studies of **BnPh$_2$** and **MePh$_2$** that reveal not only high barriers to nitrogen inversion but also unusually high barriers to isolated phenyl rotation. Molecular mechanics calculations provide insight into the origin of the high phenyl rotation barriers.

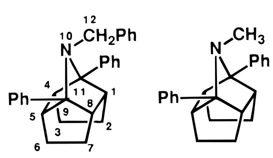

BnPh$_2$ **MePh$_2$**

X-Ray Crystallographic and Dynamic NMR Studies. The X-ray crystallographic molecular structure of **BnPh$_2$** is shown in Figure 1.[31] The molecular symmetry is C_1. The central C9–N10–C11 imine bridge bond angle of 96.4(2)° is very close to the corresponding bond angle in 5,6,7,8-tetrafluoro-9-methyl-1,4-iminonaphthalene (95°)[18] and to that associated with the COC epoxy bridge bond angle in the photodimer of 1,4-epoxy-1,4-dihydronaphthalene (96°).[19] The imine bridge CNC bond angle in **BnPh$_2$** is constrained to a small value. The benzylic phenyl group is oriented gauche to the nitrogen lone pair. The torsion angles C9–N10–C12–C13 and C11–N10–C12–C13 are −157.6(3)° and 93.8(4)°, respectively. Both bridgehead phenyl groups adopt similar orientations. The C30–C31 bond almost eclipses the C11–C4 bond (torsion angle C4–C11–C30–C31 = 2.8(6)°). The C20–C25 bond almost eclipses the C9–C5 bond (torsion angle C5–C9–C20–C25 = −3.3(6)°). The respective planes of each bridgehead phenyl group approximately bisect the C1–C11–N10 and C8–C9–N10 bond angles. The protons on ortho carbons C21 and C35 point into the open molecular cavity that exists syn to the nitrogen lone pair. The C9–C20 and C11–C30 bond lengths are 1.507(5) Å and 1.517(5) Å, respectively. The conformation of each bridgehead phenyl group is analogous to that in the equilibrium conformation of *tert*-butylbenzene in which one C–CH$_3$ bond eclipses the plane of the phenyl group.[12] Additional geometric parameters are compiled in Table 1.

Table 1. Selected Structural Parameters for the Stable, Equilibrium Conformation of BnPh$_2$ Determined by X-ray Diffraction and Calculated by the MMX Force Field

	X-ray structure[a]	MMX structure
torsion angle (deg)		
C4–C11–C30–C31	2.8(6)	−7.71
C5–C9–C20–C25	−3.3(6)	5.54
C11–N10–C12–C13	93.8(4)	88.63
C9–N10–C12–C13	−157.6(3)	−161.11
N10–C12–C13–C14	55.2(5)	58.89
bond angle (deg)		
C9–N10–C11	96.4(2)	96.03
C1–C11–C4	97.7(3)	97.19
C3–C4–C5	116.9(3)	118.00
N10–C12–C13	113.8(3)	112.32
bond length (Å)		
C9–C20	1.507(5)	1.514
C11–C30	1.517(5)	1.513
nonbonded distance (Å)		
C2–C7	2.988(6)	3.010
C3–C6	2.949(6)	2.988
C9–C11	2.209(5)	2.161

[a] See ref 30.

The ^{1}H NMR spectrum (250 MHz) of **MePh$_2$** (3% v/v in toluene-d_8) at 345 K shows aromatic proton resonances in the chemical shift range from δ 7.60 to 7.00 (Figure 2). The spectrum due to the aromatic protons is simulated accurately as an AA′CC′D spectrum (δ_A7.54, $\delta_{A'}$7.54, δ_C7.23, $\delta_{C'}$7.23, δ_D7.12, $^4J_{AA'} = {}^4J_{CC'} = 1.4$ Hz, $^3J_{AC} = {}^3J_{A'C'} = 7.5$ Hz, $^5J_{AC'} = {}^5J_{A'C} = 0.6$ Hz, $^4J_{AD} = {}^4J_{A'D} = 1.4$ Hz, $^3J_{CD} = {}^3J_{C'D} = 7.5$ Hz).[20] The full five-spin simulation is illustrated in the upper right corner of Figure 2. On the basis of this analysis, the A and A′ resonances are assigned logically to the ortho protons, the C and C′ signals to the meta protons, and the D multiplet to the para proton. In the aliphatic region of the spectrum at 345 K (Figure 3), there are signals due to the methine protons at δ 2.56 (broadened signal showing no resolved fine structure), the *N*-methyl group at δ 1.72 (singlet), and the methylene protons at δ 1.70–1.50 (complex multiplet reflecting diastereotopic *exo* and *endo* protons).

At temperatures below 345 K, the resonances due to the methine and methylene protons decoalesce while the *N*-methyl singlet remains unchanged (Figure 3). This decoalescence is consistent with slowing inversion at nitrogen (Scheme 1). As a result of inversion, the methyl group exchanges between two equivalent molecular environments. As inversion slows, the methyl signal will not decoalesce, as observed. The methine and methylene protons, respectively, exchange between diastereotopic molecular environments alternately syn and anti to the methyl group. The decoalesced spectrum at 205 K (Figure 3) does indeed show two methine proton resonances at δ_M 2.54 and δ_N 2.40 and two methylene multiplets at δ 1.68 and 1.32, reflecting methine and

(17) Gribble, G. W.; Easton, N. R., Jr.; Eaton, J. T. *Tetrahedron Lett.* **1970**, 1075.
(18) Byrn, M. P.; Strouse, C. E.; Gribble, G. W.; LeHoullier, C. S. *Acta Crystallogr.* **1985**, *C41*, 238.
(19) Bordner, J.; Stanford, R. H.; Dickerson, R. E. *Acta Crystallogr.* **1970**, *B26*, 1126.
(20) Harris, R. K.; Woodman, C. M. *QCPE* **1966**, Program No. 188. Harris, R. K.; Woodman, C. M. *Mol. Phys.* **1966**, *10*, 437.

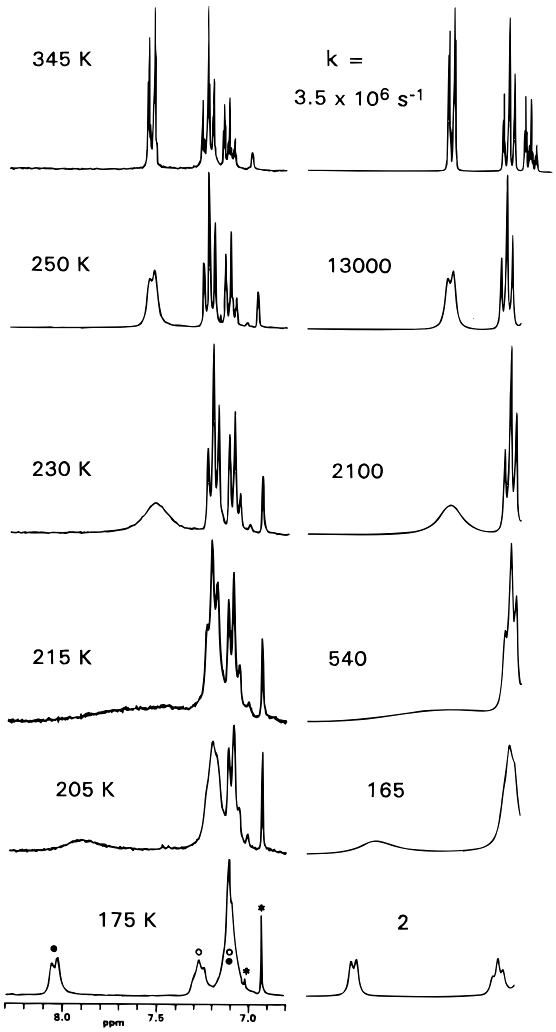

Figure 2. ^{1}H DNMR spectra (250 MHz) due to the aromatic protons of **MePh$_2$** (3% v/v in toluene-d_8) in the left column and theoretical simulations in the right column. The rate constant is associated with phenyl rotation. The rate constant at 345 K was obtained by extrapolation of values from lower temperatures. The solid circles on the 175 K spectrum indicate the location of the resonances due to the two diastereotopic ortho protons. The open circles indicate the location of the resonances due to the two diastereotopic meta protons. The asterisked peaks are due to proton isotopic impurities in toluene-d_8 that sharpen at lower temperatures due to increasingly efficient deuterium quadrupolar relaxation effectively spin decoupling deuterium.

methylene protons that are, respectively, syn and anti to the methyl group and reflecting slow inversion.

A rigorous theoretical simulation of the dynamic NMR (DNMR) spectra of the aliphatic protons in Figure 3 requires exchange of magnetization between two 12-spin spectra. This is well beyond the capability of current DNMR line shape computer programs. However, as shown in Figure 3, good theoretical fits of the DNMR spectra due to the methine protons were obtained by employing a simplified DNMR model that involves exchange between MM′XX′ (δ_M 2.54, $\delta_{M'}$ 2.54, δ_X 1.68, $\delta_{X'}$ 1.68, $J_{MM'} = 7.8$ Hz, $J_{MX} = J_{M'X'} = 4.5$ Hz, $J_{M'X} = J_{MX'} = 1.0$ Hz, $J_{XX'} = 0$ Hz) and NN′ZZ′ (δ_N 2.40, $\delta_{N'}$ 2.40, δ_Z 1.32, $\delta_{Z'}$ 1.32, $J_{NN'} = 7.5$ Hz, $J_{NZ} = J_{N'Z'} = 4.0$ Hz, $J_{N'Z} = J_{NZ'} = 1.0$ Hz, $J_{ZZ'} = 0$ Hz) spin systems.[21] The M and M′ chemical shifts and the N and N′ chemical shifts are assigned, respectively, to the diastereotopic pairs of

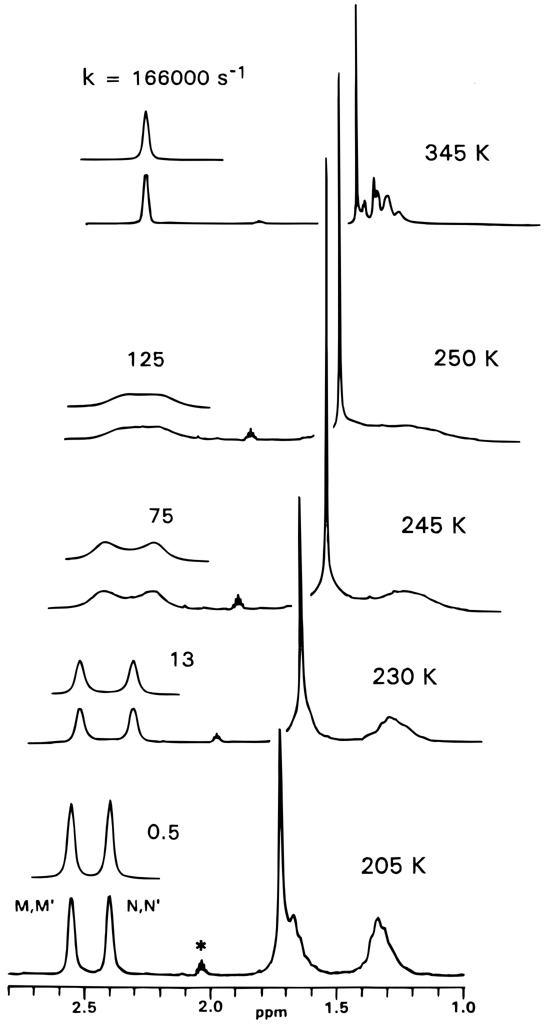

Figure 3. ^{1}H DNMR spectra (250 MHz) due to the aliphatic protons of **MePh$_2$** (3% v/v in toluene-d_8) and theoretical simulations. For clarity, the spectra are progressively offset to the right with increasing temperature. The rate constant is associated with nitrogen inversion. The asterisked multiplet is due to a proton isotopic impurity in toluene-d_8.

methine protons in a given conformation (Scheme 1). The activation parameters for nitrogen inversion derived from the simulations are $\Delta H^‡ = 12.4 \pm 0.4$ kcal/mol, $\Delta S^‡ = 0.8 \pm 2$ cal/mol K, and $\Delta G^‡ = 12.2 \pm 0.1$ kcal/mol at 250 K. Activation parameters for nitrogen inversion are also listed in Table 2.

As shown in Figure 2, the resonance due to the ortho protons on the phenyl groups of **MePh$_2$** decoalesces into two widely spaced signals at δ_A 8.05 and δ_D 7.10 indicated by solid circles in the 175 K spectrum. The resonance due to the meta protons also decoalesces into two signals at δ_B 7.28 and δ_C 7.13 indicated by open circles in the 175 K spectrum. One ortho proton resonance, one meta proton resonance, and the para proton signal are superimposed at δ 7.1. This decoalescence is assigned to slowing phenyl rotation (Scheme 1) and constitutes the rare observation of a phenyl rotation barrier that is high enough to be DNMR-visible.[9] A rigorous simulation of the DNMR spectra due to the phenyl groups requires exchange between two 5-spin spectra both of which contain five unique chemical shifts. This problem is also

(21) Brown, J. H.; Bushweller, C. H. *QCPE* **1993**, Program No. 633. For a PC-based program used to plot the DNMR spectra, see: Brown, J. H. *QCPE* **1993**, Program No. QCMP 123.

Scheme 1

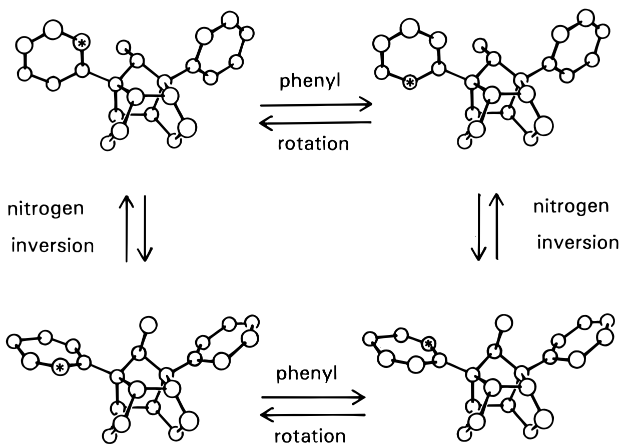

Table 2. Activation Parameters for Nitrogen Inversion and Phenyl Rotation

	nitrogen inversion		
compd[a]	$\Delta H^\ddagger$, kcal/mol	$\Delta S^\ddagger$, cal/mol-K	$\Delta G^\ddagger$, kcal/mol (T, K)
$MePh_2$	12.4 ± 0.4	0.8 ± 2	12.2 ± 0.1 (250)
$BnPh_2$	11.6 ± 0.4	4.6 ± 2	10.6 ± 0.1 (215)
	phenyl rotation		
compd	$\Delta H^\ddagger$, kcal/mol	$\Delta S^\ddagger$, cal/mol-K	$\Delta G^\ddagger$, kcal/mol (T, K)
$MePh_2$	9.5 ± 0.4	−1.4 ± 2	9.8 ± 0.1 (210)
$BnPh_2$	9.4 ± 0.4	−1.6 ± 2	9.8 ± 0.1 (210)

[a] Solvent is toluene-d_8.

beyond the capability of current DNMR line shape computer programs. However, excellent fits of the DNMR spectra over the chemical shift ranging from δ 8.20 to 7.20 were achieved by employing exchange between ABE (δ_A 8.05, δ_B 7.28, δ_E 7.10, $^3J_{AB} = 7.8$ Hz, $^4J_{AE} = 1.4$ Hz, $^3J_{BE} = 7.4$ Hz) and DCE (δ_D 7.10, δ_C 7.13, δ_E 7.10, $^3J_{CD} = 7.8$ Hz, $^4J_{DE} = 1.4$ Hz, $^3J_{CE} = 7.4$ Hz) spin systems.[21] Simulations at 250 K and at lower temperatures are illustrated in Figure 2. The activation parameters for phenyl rotation are $\Delta H^\ddagger = 9.5 \pm 0.4$ kcal/mol, $\Delta S^\ddagger = -1.4 \pm 2$ cal/mol-K, and $\Delta G^\ddagger = 9.8 \pm 0.1$ kcal/mol at 210 K, revealing a barrier to phenyl rotation that is lower than that for nitrogen inversion. At 230 K, phenyl rotation occurs at a rate 160 times faster than nitrogen inversion. The two processes occur separately; they are not concerted.[1]

The ^{1}H NMR spectrum (250 MHz) of **BnPh$_2$** (3% wt/v in toluene-d_8) at 300 K shows a series of complex aromatic proton resonances in the chemical shift range from δ 7.50 to 6.70 (Figure 4). An ^{1}H DQF-COSY spectrum (500 MHz) recorded by using the pulse sequence of Rance et al. established connectivities in the phenyl groups.[22] There are two isolated subspectra that do not overlap; one has resonances in the range δ 7.50−6.94, the other from δ 6.94 to 6.70. The ratio of the integrated intensities of the first subspectrum to the second is 2:1. The first subspectrum must be assigned to the bridgehead phenyl groups and the second to the phenyl group on the benzyl substituent. The subspectrum due to the bridgehead phenyl groups is simulated accurately as an AA′CC′D spectrum (δ_A 7.45, $\delta_{A'}$ 7.45, δ_C 7.09, $\delta_{C'}$ 7.09, δ_D 7.02, $^4J_{AA'} = {}^4J_{CC'} = 1.5$ Hz, $^3J_{AC} = {}^3J_{A'C'} = 7.6$ Hz, $^5J_{AC'} = {}^5J_{A'C} = 0.2$ Hz, $^4J_{AD} = {}^4J_{A'D} = 1.5$ Hz, $^3J_{CD} = {}^3J_{C'D} = 7.6$ Hz).[20] In a manner exactly analogous to **MePh$_2$** (*vide supra*), the A and A′ resonances are assigned to the ortho protons, the C and C′ signals to the meta protons, and the D multiplet to the para proton. The subspectrum due to the benzylic group is simulated accurately as an EE′FGG′ spectrum (δ_E 6.88, $\delta_{E'}$ 6.88, δ_F 6.86, δ_G 6.76, $\delta_{G'}$ 6.76, $^4J_{EE'} = {}^4J_{GG'} = 1.4$ Hz, $^3J_{EF} = {}^3J_{E'F} = 7.6$ Hz, $^3J_{EG} = {}^3J_{E'G'} = 7.6$ Hz, $^5J_{EG'} = {}^5J_{E'G} = 0.2$ Hz, $^4J_{FG} = {}^4J_{FG'} = 1.4$).[20] On the basis of this analysis, the G and G′ resonances are assigned logically to the ortho protons, the E and E′ signals to the meta protons, and the F resonance to the para proton. A complete simulation of the aromatic protons spectrum incorporating both subspectra is illustrated at the upper right corner of Figure 4.

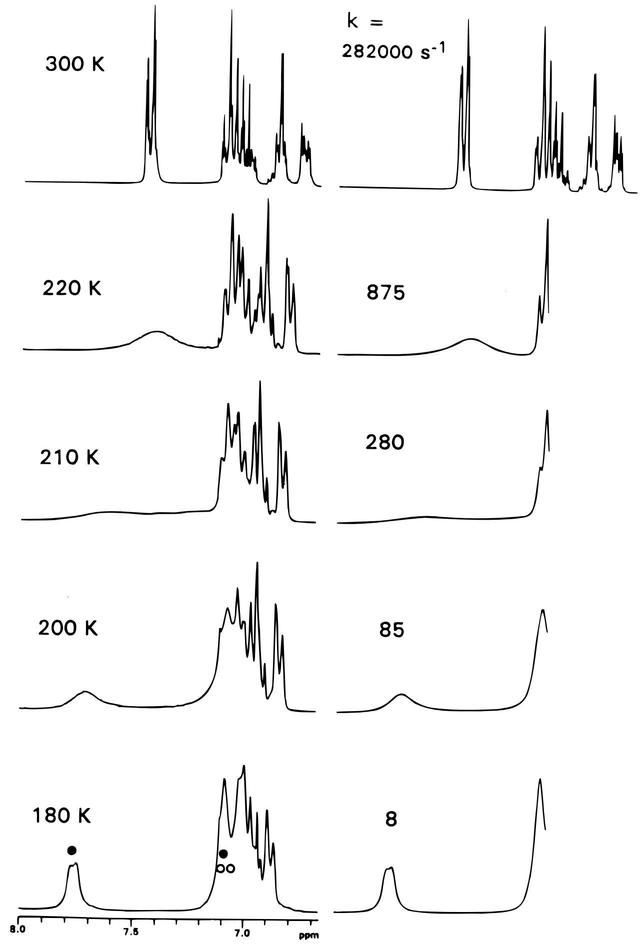

Figure 4. ^{1}H DNMR spectra (250 MHz) due to the aromatic protons of **BnPh$_2$** (3% wt/v in toluene-d_8) in the left column and theoretical simulations in the right column. The rate constant is associated with bridgehead phenyl rotation. The rate constant at 300 K was obtained by extrapolation of values from lower temperatures. The solid circles on the 180 K spectrum indicate the location of the resonances due to the two diastereotopic ortho protons. The open circles indicate the location of the resonances due to the two diastereotopic meta protons.

In the aliphatic region of the spectrum of **BnPh$_2$** at 300 K (Figure 5), there are resonances due to the benzylic protons at δ 3.18 (singlet), the methine protons at δ 2.60 (broadened signal showing no resolved fine structure), and the methylene protons at δ 1.72−1.45. At temperatures below 300 K, the signals due to the methine and methylene protons decoalesce while the benzylic protons singlet remains unchanged, consistent with slowing inversion at nitrogen (*vide supra*). In a manner analo-

(22) Rance, M.; Sorensen, O.; Bodenhausen, G.; Wagner, G.; Ernst, R. R.; Wuthrich, K. *Biochem. Biophys. Res. Commun.* **1983**, *117*, 479.

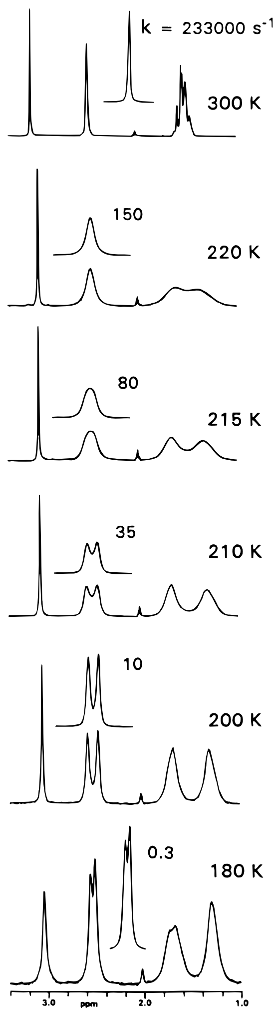

Figure 5. ^{1}H DNMR spectra (250 MHz) due to the aliphatic protons of **BnPh$_2$** (3% wt/v in toluene-d_8) and theoretical simulations. The rate constant is associated with nitrogen inversion.

gous to **MePh$_2$**, good theoretical fits of the DNMR spectra due to the methine protons were obtained by invoking exchange between MM′XX′ (at 180 K: δ_M 2.55, $\delta_{M'}$ 2.55, δ_X 1.70, $\delta_{X'}$ 1.70, $J_{MM'}$ = 8.0 Hz, J_{MX} = $J_{M'X'}$ = 5.0 Hz, $J_{M'X}$ = $J_{MX'}$ = 2.0 Hz, $J_{XX'}$ = 0) and NN′ZZ′ (at 180 K: δ_N 2.50, $\delta_{N'}$ 2.50, δ_Z 1.30, $\delta_{Z'}$ 1.30, $J_{NN'}$ = 7.5 Hz, J_{NZ} = $J_{N'Z'}$ = 4.0 Hz, $J_{N'Z}$ = $J_{NZ'}$ = 1.0 Hz, $J_{ZZ'}$ = 0 Hz) spin systems.[21] In fitting the DNMR spectra, it is necessary to incorporate a progressive upfield shift of the N and N′ resonances with increasing temperature (Figure 5). The activation parameters for nitrogen inversion are $\Delta H^{\ddagger} = 11.6 \pm 0.4$ kcal/mol, $\Delta S^{\ddagger} = 4.6 \pm 2$ cal/mol-K, $\Delta G^{\ddagger} = 10.6 \pm 0.1$ kcal/mol at 215 K. Inversion is more facile in **BnPh$_2$** than in **MePh$_2$** (Table 2).

As shown in Figure 4, the resonances due to the aromatic protons on the benzyl group show no evidence of decoalescence down to 180 K. In contrast, the signal due to the ortho protons on the bridgehead phenyl groups shows a clear-cut decoalescence analogous to that observed for **MePh$_2$** consistent with slowing phenyl rotation. By using a DNMR exchange model that is strictly analogous to that used for **MePh$_2$** (*vide supra*), the spectral region from δ 8.00 to 7.06 for **BnPh$_2$** is simulated accurately by employing exchange between ADE (δ_A7.76, δ_D7.04, δ_E7.00, $^3J_{AD}$ = 7.4 Hz, $^4J_{AE}$ = 1.4 Hz, $^3J_{DE}$ = 7.4 Hz) and CBE (δ_C 7.08, δ_B 7.10, δ_E 7.00, $^3J_{CB}$ = 7.4 Hz, $^4J_{CE}$ = 1.4 Hz, $^3J_{BE}$ = 7.4 Hz) spin systems (Figure 4).[21] The activation parameters for bridgehead phenyl rotation are $\Delta H^{\ddagger} = 9.4 \pm 0.4$ kcal/mol, $\Delta S^{\ddagger} = -1.6 \pm 2$ cal/mol-K, and $\Delta G^{\ddagger} = 9.8 \pm 0.1$ kcal/mol at 210 K. The barriers to bridgehead phenyl rotation in **MePh$_2$** and **BnPh$_2$** are essentially identical. In **BnPh$_2$**, the differential between the barriers to nitrogen inversion and phenyl rotation is smaller than that in **MePh$_2$**; in **BnPh$_2$** at 210 K, phenyl rotation occurs at a rate only eight times faster than inversion.

It is reasonable to assume that the bridgehead phenyl groups in **MePh$_2$** adopt conformational preferences analogous to those in **BnPh$_2$**. Scheme 1 illustrates the nitrogen inversion process in **MePh$_2$**. When inversion occurs, e.g., upper left to lower left structure in Scheme 1, each phenyl group must reorient via a small torsion about the phenyl to cage bond. In the upper left structure, the bond between the phenyl quaternary carbon and the asterisked ortho carbon essentially bisects the molecular cavity syn to the lone pair and, after inversion, ends up essentially eclipsing a carbon−carbon bond in the cage. While the inversion barrier is substantial (*vide supra*), the barrier associated with this phenyl torsion will be minuscule. The process is strictly analogous to the very facile 6-fold *tert*-butyl rotation in *tert*-butylbenzene.[12] This inversion−torsion process is sufficient to interchange the ortho and meta carbons between their respective diastereotopic molecular environments. Scheme 1 also illustrates that a 180° isolated rotation of phenyl *with no inversion* will also interchange the ortho and meta carbons, respectively, between diastereotopic molecular environments (Scheme 1). Both processes (inversion−torsion and a 180° isolated phenyl rotation) are sufficient to interchange the molecular environments of the ortho and meta carbons. If the inversion−torsion process remains fast on the NMR chemical exchange time scale, the 180° isolated phenyl rotation will always be invisible to the DNMR method no matter how high the phenyl rotation barrier. If the 180° isolated phenyl rotation barrier is higher than that for inversion−torsion, simultaneous decoalescence of the aromatic and aliphatic protons signals will occur only when nitrogen inversion (lower barrier) slows on the DNMR time scale.[1] If the 180° isolated phenyl rotation barrier is lower than that for inversion−torsion, separate decoalescence phenomena over different temperature ranges due to the two different processes will be observed. This is the actual situation (*vide supra*).

Pyramidal inversion at the nitrogen atom of a sterically unencumbered acyclic trialkylamine is facile.[1] The free energy of activation for inversion in diethylmethylamine is 7.9 kcal/mol at 160 K.[23] In contrast, incorporation of the nitrogen atom into a rigid multicyclic framework that constrains a CNC bond angle in the transition state for inversion to some value much less than 120° generates significant angle strain in the transition state and induces a significant increase in the barrier to inversion.[2−4] The inversion barrier in 7-methyl-7-azanorbornane is 13.8 kcal/mol.[3] The barriers to inversion in **MePh$_2$** and **BnPh$_2$** are consistent with substantial angle strain in the transition state for inversion. However, Malpass has proposed that the main origin of this barrier-raising "bicyclic effect" on nitrogen inversion is due to delocalization of the nitrogen lone pair into the bicyclic frame-

(23) Bushweller, C. H.; Fleischman, S. H.; Grady, G. L.; McGoff, P.; Rithner, C. D.; Whalon, M. R.; Brennan, J. G.; Marcantonio, R. P.; Domingue, R. P. *J. Am. Chem. Soc.* **1982**, *104*, 6224.

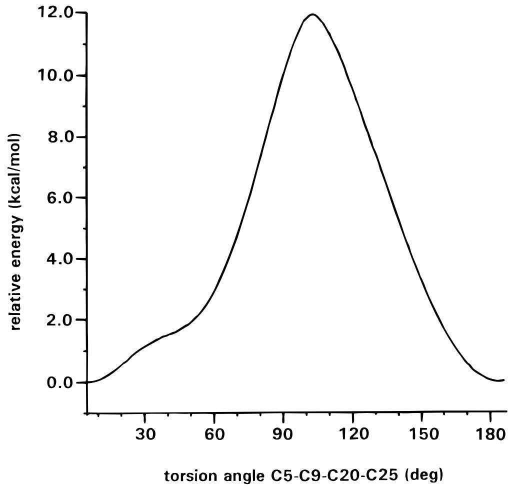

Figure 6. Energy profile for rotation of the C20 phenyl group in **MePh$_2$** (see **2**) calculated using the torsion angle driver option (1° increments) in the MMX force field.[24,25]

work leading to unusual ground state stabilization.[8] Consistent with this theory is the observed dramatic deshielding of the nitrogen atom in the ^{15}N NMR spectra of 7-azabicyclo[2.2.1]heptyl compounds.[8] In any event, further work is needed to diagnose the relative importance of the various structural and electronic contributions to this interesting "bicyclic effect" on nitrogen inversion.

Barriers to rotation about sp^3−sp^2 carbon−carbon bonds in simple, unencumbered molecules are usually too low to be DNMR-detectable.[9,10] The barrier to methyl rotation in toluene is 0.014 kcal/mol.[11] Gas-phase electron-diffraction studies indicate that *tert*-butylbenzene prefers that conformation with one C−Me bond eclipsing the phenyl plane.[12] The calculated transition state for *tert*-butyl rotation has a C−Me bond in a plane perpendicular to the phenyl plane and is computed to be only 0.5−0.7 kcal/mol above the equilibrium geometry.[12] In light of these data, the high phenyl rotation barriers in **MePh$_2$** and **BnPh$_2$** are remarkable.

Molecular Mechanics Calculations

In order to provide some insight into the origin of the unusually high phenyl rotation barriers, molecular mechanics calculations using the MMX force field were performed.[24] For **BnPh$_2$**, one of four equivalent or enantiomeric MMX minimum energy equilibrium conformations (C_1 symmetry) is shown below (see structure **1**).

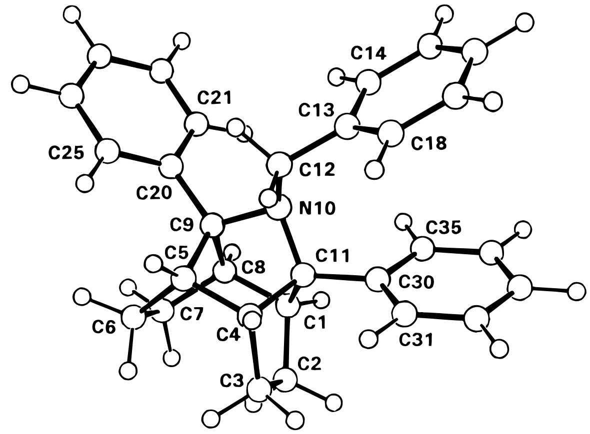

1

A visual comparison of **1** and the crystal molecular conformation in Figure 1 and a perusal of selected structural parameters in Table 1 show good agreement between the X-ray and calculated structures.

As expected, the MMX minimum energy equilibrium conformation of **MePh$_2$** has C_s symmetry (**2**). The calculated torsion angles C4−C11−C30−C31 and C5−C9−C20−C25 in **2** are −5.17° and 5.15°, respectively.

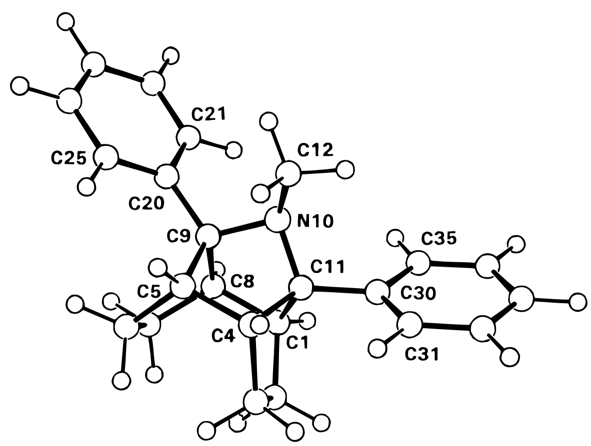

2

MMX torsion angle driver calculations (1° increments) were performed to generate energy profiles for phenyl rotation.[25] The profile for rotation of the C20 phenyl group of **MePh$_2$** (see **2**) is illustrated in Figure 6. Proceeding from left to right along the C5−C9−C20−C25 torsion angle axis in Figure 6 corresponds to a counterclockwise rotation of phenyl looking down the C20−C9 bond. The lower energy inflection at a torsion angle of about 30° corresponds to a conformation analogous to the transition state for 6-fold *tert*-butyl rotation in *tert*-butylbenzene; the C9−N10 bond is located in a plane perpendicular to the phenyl plane. As rotation continues, the energy rises significantly to a transition state in which the C5−C9−C20−C25 and N10−C9−C20−C25 torsion angles are 102.95° and −23.55°, respectively. Two perspectives of that transition state are shown below (see **3a** and **3b**). The calculated barrier is 11.91 kcal/mol. In transition state **3**, it is clear that *o*-phenyl protons are, respectively, in close passage with the methyl group and the *exo* methylene proton on C7. In order to optimize

(24) MMX calculations were performed with program PCMODEL, PX5 version (2/6/95), Serena Software, Bloomington, IN. Geometry optimization for all equilibrium conformations was done with true π-atoms (with periodic SCF-π minimization).[25] See: Gajewski, J. J.; Gilbert, K. K.; McElvey, J. *Advances in Molecular Modeling*; JAI Press: Greenwich, CT, 1992; Vol. 2. The ORTEP drawings were produced with PCDISPLAY, Serena Software, Bloomington, IN.

(25) In our efforts to generate energy profiles for phenyl rotation using MMX torsion angle driver calculations, employing true π-atoms (with periodic SCF-π minimization) frequently produced spurious "spikes" at or near the transition state energies. However, employing "CA" atoms for the phenyl carbons gave substantially more continuous energy profiles. The "CA" carbon atoms have a fixed trigonal planar geometry, fixed C−H bond lengths, and fixed C−C bond lengths. SCF calculations are not performed when "CA" atoms are used. For example, an MMX torsion angle driver calculation (using "CA" phenyl carbons) for *tert*-butyl rotation in *tert*-butylbenzene gave a symmetric, continuous energy profile for the 6-fold rotation and a barrier (0.61 kcal/mol) in excellent agreement with previous calculations.[12] The use of true π-atoms resulted in a seriously asymmetric set of barriers over a 360° rotation and "spikes" as high as 3 kcal/mol. Therefore, all barrier calculations reported here were performed with "CA" atoms for the phenyl group.

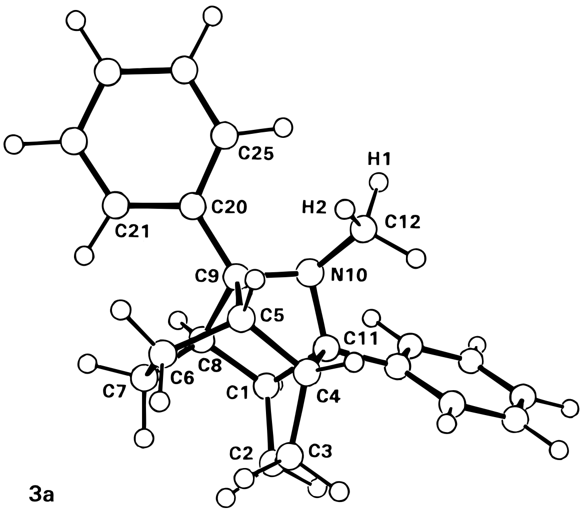

3a

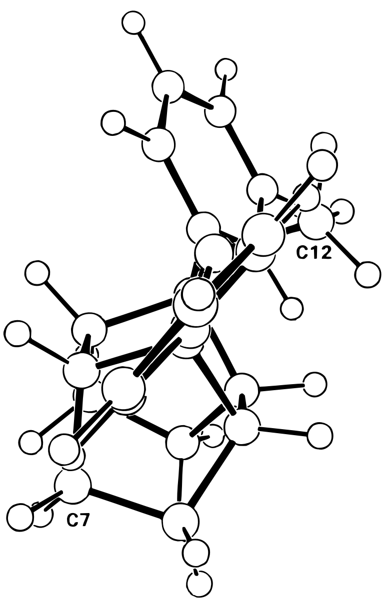

3b

nonbonded repulsions, the methyl group rotates away from a classic staggered orientation and the cage distorts. The H_{exo}−C7−C6−H_{exo} torsion angle in **3** is −18.86° and the C20−C9−N10 bond angle is 115.64° as compared to 2.27° and 112.86°, respectively, in the equilibrium conformation **2**. In **3a**, the distances between the proton on C25 and the H1 and H2 methyl protons are 2.06 Å and 2.29 Å, respectively. The distance between the proton on C21 and the *exo* methylene proton on C7 is 2.00 Å.

While the two bridgehead phenyl groups in the equilibrium conformation of **BnPh₂** are diastereotopic (Figure 1 and structure **1**), the DNMR spectra down to 180 K show just one subspectrum for these groups. In addition, the signal due to the benzylic methylene protons remains a singlet down to 180 K. This is consistent with rapid isolated rotation about the N−CH_2 bond that interconverts three equilibrium rotamers (two enantiomeric forms each with the phenyl group gauche to the lone pair; one with the phenyl group anti to the lone pair). MMX barrier calculations support this hypothesis. The MMX barrier for conversion of **1** to its enantiomer (phenyl passes the lone pair) is a minuscule 1.42 kcal/mol consistent with very rapid equilibration that is typical of such processes.[1] This very low barrier is due in part to a torsion about the N−CH_2 bond in the stable equilibrium conformation **1** that moves the phenyl group away from classic staggering toward the lone pair and toward the transition state for rotation. The calculated C11−N10−C12−C13 torsion angle in **1** is 88°; the same torsion angle in the crystal molecular structure is 93.8-(4)°. Rotation of the benzyl group from the gauche orientation in **1** to the conformation in which the phenyl group is anti to the lone pair (**4**) involves an MMX barrier equal to 6.16 kcal/mol. Conformation **4** (torsion angle

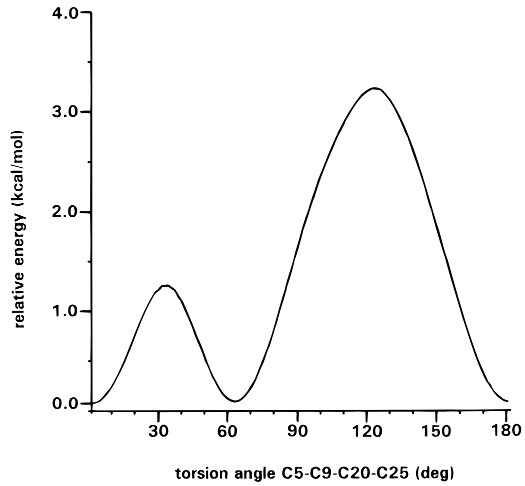

Figure 7. Energy profile for rotation of the C20 phenyl group in **HPh₂** (see **5**) calculated using the torsion angle driver option (1° increments) in the MMX force field.[24,25]

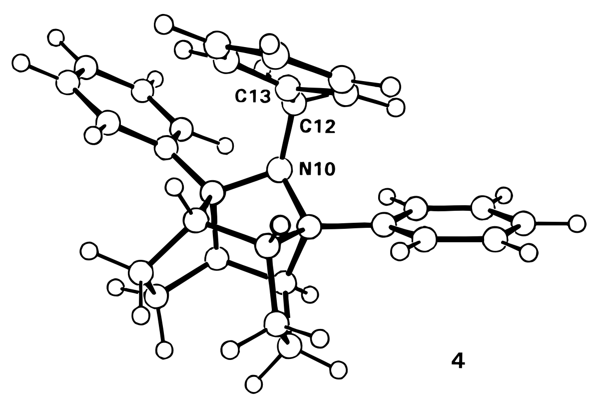

4

Lp−N10−C12−C13 = −171.18°) is calculated to be 3.7 kcal/mol higher in energy than **1**; **4** will be present at such a minuscule concentration that it is irrelevant to any discussion of the stereodynamics of **BnPh₂**.

The MMX-calculated barrier for rotation about the N−CH_2 bond in **BnPh₂** during which the benzyl phenyl group passes the lone pair is a minuscule 1.4 kcal/mol. This is close to a free interconversion of the two enantiomers. Therefore, during the course of bridgehead phenyl rotation, an energy-optimizing reorientation of the benzyl group will be extremely facile. A reasonable transition state for rotation of the C20 bridgehead phenyl group in Figure 1 would involve orienting the benzyl group close to the conformation shown in Figure 1. The nonbonded interactions in the transition state for C20 phenyl rotation in **BnPh₂** would be virtually identical to those in the transition state for phenyl rotation in **MePh₂** (see **3a,b**). The barriers to bridgehead phenyl rotation in **BnPh₂** and **MePh₂** should be very similar, as observed (Table 2). Consistent with this rationale, we computed the MMX barrier for rotation of the C20 bridgehead phenyl group in with the benzyl group oriented as shown in **1**. The MMX barrier is 12.02 kcal/mol via a transition state that is strictly analogous to **3**.

It is apparent from the MMX barrier calculations for **MePh₂** and **BnPh₂** that the origin of the unusually high phenyl rotation barriers is the extremely close passage of *o*-phenyl and *N*-alkyl protons in the transition state (e.g., **3**). As a test of this rationale, the phenyl rotation barrier in the demethyl derivative (**HPh₂**) was calculated using the MMX torsion angle driver option. In one stable equilibrium conformation of **HPh₂** (**5**; C_s symmetry), the

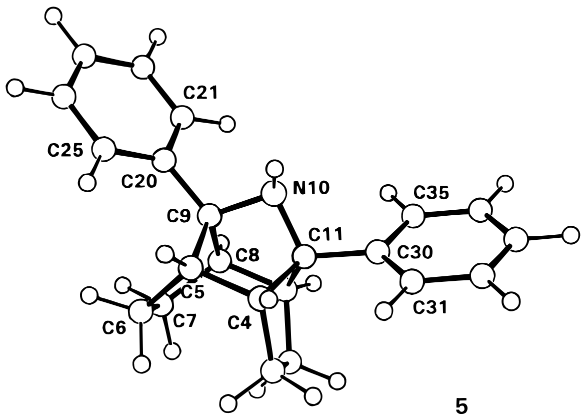

5

calculated C4−C11−C30−C31 and C5−C9−C20−C25 torsion angles are −2.74° and 2.43°, respectively. Starting from **5**, Figure 7 illustrates the MMX energy profile (1° increments) for rotation of the C20 phenyl group. Proceeding fom left to right along the C5−C9−C20−C25 torsion angle axis in Figure 7 corresponds to a counterclockwise rotation of phenyl looking down the C20−C9 bond. The first maximum at a C5−C9−C20−C25 torsion angle equal to 34° ($\Delta H^{\ddagger}_{\mathrm{MMX}} = 1.18$ kcal/mol) corresponds to a conformation analogous to the transition state for 6-fold *tert*-butyl rotation in *tert*- butylbenzene; the C9−N10 bond is located in a plane perpendicular to the phenyl plane. As shown in Figure 7, another stable equilibrium conformation exists at a C5−C9−C20−C25 torsion angle equal to 64°. In this conformation, the C20−C21 bond eclipses the C9−C8 bond. These two conformations are computed to be essentially equal in energy, suggesting of course, that **HPh₂** exists as four essentially equally populated equilibrium conformations (a pair of enantiomers having phenyl groups twisted in different senses and two diastereomeric conformations each having C_s symmetry). Continuing the phenyl rotation (Figure 7) produces another higher energy transition state at a C5−C9−C20−C25 torsion angle equal to 124° ($\Delta H^{\ddagger}_{\mathrm{MMX}} = 3.13$ kcal/mol). Two perspectives of that transition state are shown below (**6a** and **6b**). In **6a** or **6b**, the N10−C9 and C20−C25 bonds are nearly eclipsed (torsion angle N10−C9−C20−C25 = 1.86°). The orientation of the C20 phenyl group in this transition state and the shape of the energy profile in Figure 7 suggest that the N−H proton is essentially invisible to the rotating phenyl group. The salient observation is that the barrier to phenyl rotation in **HPh₂** is calculated to be *8.8 kcal/mol lower* than that in **MePh₂**. In this transition state, there is significantly less cage distortion (torsion angle H_{exo}−C7−C6−H_{exo} = 2.33°; bond angle C20−C9−N10 = 111.74°) than in the transition state for **MePh₂** (see **3**). It is apparent that the sterically minuscule N−H proton in **HPH₂** allows considerably more freedom for molecular

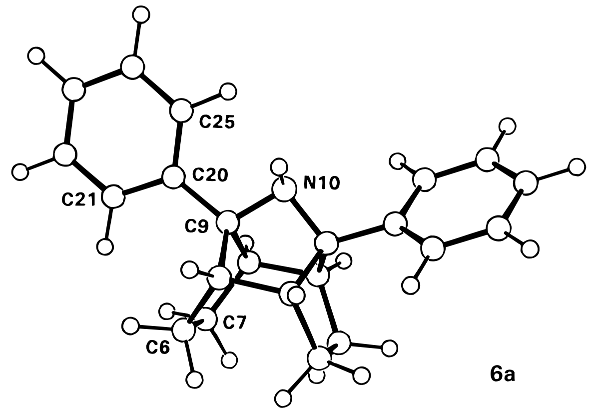

6a

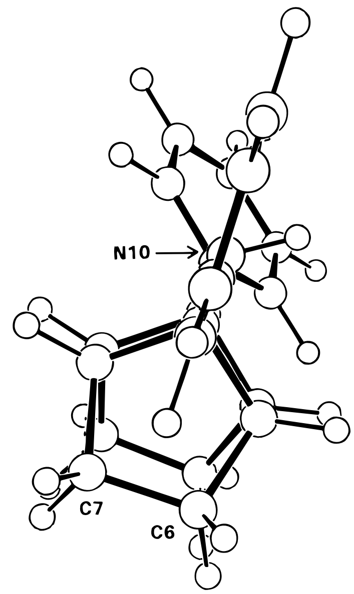

6b

reorganization in optimizing nonbonded repulsions in conformations along the phenyl rotation pathway. This would seem to confirm that the unusually high barriers to phenyl rotation in **MePh₂** and **BnPh₂** are due to the required very close passage of an *o*-phenyl proton and a methyl proton in the transition state.

MePh₂ and **BnPh₂** are molecules that have rigid molecular frameworks. In such systems, substituents can be highly constrained. Substituent stereodynamics can be significantly altered compared to the same substituents on more flexible frameworks. This is exemplified by the high phenyl rotation and nitrogen inversion barriers in **MePh₂** and **BnPh₂**.

Experimental Section

NMR Spectra. The dynamic NMR spectra were recorded by using a Bruker WM-250 NMR system at the University of Vermont. NMR sample temperature was varied by using a custom-built nitrogen gas delivery system used in conjunction with a Bruker BVT-1000 temperature control unit. Temperature measurement is accurate to ±1 K. NMR samples were prepared in precision 5-mm tubes. All spectra are referenced to tetramethylsilane at 0 ppm. The 500 MHz ^{1}H NMR spectra were recorded by using a Varian Unity plus NMR system at Dartmouth College. The DQF-COSY spectra were recorded by using the sequence of Rance et al.[22] with the addition of a homospoil-90-homospoil sequence at the beginning of the relaxation delay which gives a less oscillatory steady state when the recycle time is shorter than T_1. All measurements were carried out in toluene-d_8 at 298 K. All experiments were executed in the phase-sensitive mode with phase incrementation of the first pulse according to the method of States et al.[26] Quadrature detection was employed in both dimensions, and the carrier was placed in the center of the spectrum. The spectral width was 4500 Hz in both directions. A total of 512 complex points were collected in t_1. The 2D data sets were multiplied in both dimensions by phase-shifted sine-bell functions, zero-filled, and Fourier transformed to 2048 points in t_2 and 1024 points in t_1.

Crystal Structure Determination. 10-Benzyl-9,11-diphenyl-10-azatetracyclo[6.3.0.0.^{4,11}0.^{5,9}]undecane (**BnPh$_2$**) crystallized from hexane as white needles in the monoclinic system *Pn*. Unit cell dimensions are as follows: $a = 12.198(1)$ Å, $b = 6.1399(6)$ Å, $c = 14.938(2)$ Å, $\beta = 107.470(4)°$, $V = 1067.1(2)$ Å^3, $Z = 2$. The crystal was examined on a Huber (Crystal Logic) diffractometer, Mo Kα radiation, at 298 K. A total of 3517 reflections and 1737 with $I > 3\sigma(I)$ was collected. The structure was determined by direct methods. Full-matrix least-squares refinement based on *F* of 271 parameters has an agreement value, *R*, of 0.047 and a weighted *R* of 0.051. The error of fit is 1.595, and the maximum residual density is 0.32 e/Å^3. All of the non-hydrogen atoms were refined anisotropically. The hydrogen atom positions were calculated near the end of the refinement, and the *xyz* parameters were shifted in further refinements based on the carbon to which they are attached. A single parameter was refined corresponding to the temperature factor of all the hydrogen atoms.

Compound Syntheses. The full synthetic details will be reported separately. The general method follows. The syntheses of 10-benzyl-9,11-diphenyl-10-azatetracyclo[6.3.0.0.^{4,11}0.^{5,9}]undecane (**BnPh$_2$**) and 10-methyl-9,11-diphenyl-10-azatetracyclo[6.3.0.0.^{4,11}0.^{5,9}]undecane (**MePh$_2$**) were performed by employing the general methods of Anderson and Heider for the preparation of mesoionic 1,3-oxazolium-5-olates ("munchnones")[27] and of Weintraub[28] for the tandem cycloaddition reaction of 1,5-cyclooctadiene and sydnones. A mixture of excess 1,5-cyclooctadiene (5 mL) and *N*-benzoyl-*N*-benzylphenylglycine[29] (5 mmol) (or *N*-benzoyl-*N*-methylphenylglycine) was treated with diisopropylcarbodiimide (5 mmol) under nitrogen at room temperature with magnetic stirring. The mixture was heated at reflux for 15 min, cooled to room temperature, diluted with ether (50 mL), and filtered. The filtrate was extracted with 5% aqueous HCl (2 × 100 mL). The acid layer was diluted with ice (50 g) and CH_2Cl_2 (100 mL) and rendered basic with NaOH pellets (ice bath cooling). The CH_2Cl_2 extract was dried (Na_2SO_4) and concentrated in vacuo. The residue was triturated with hexane to remove insoluble urea byproduct. The desired product was either crystallized from hexane or purified by flash chromatography (silica gel) to give **BnPh$_2$** and **MePh$_2$** in 57% and 74% yields, respectively.

Both compounds exhibited satisfactory spectral and analytical data.

10-Benzyl-9,11-diphenyl-10-azatetracyclo[6.3.0.0.^{4,11}0.^{5,9}]undecane (BnPh$_2$): mp 167−168 °C (hexane); ^{1}H NMR ($CDCl_3$) δ 7.50 (m, 4H), 7.15 (m, 7H), 6.84 (m, 2H), 6.57 (m, 2H), 3.20 (s, 2H), 2.74 (s, 4H), 1.64 (m, 4H) ppm; ^{13}C NMR ($CDCl_3$) δ 141.8, 139.9, 128.6, 128.2, 127.7, 126.9, 126.8, 125.0, 83.9, 50.5, 47.3, 23.1 ppm; MS *m/e* 391, 301, 91.

Anal. Calcd for $C_{29}H_{29}N$: C, 88.96; H, 7.47; N, 3.58. Found: C, 88.84, H, 7.44; N, 3.54.

10-Methyl-9,11-diphenyl-10-azatetracyclo[6.3.0.0.^{4,11}0.^{5,9}]undecane (MePh$_2$): oil; ^{1}H NMR ($CDCl_3$) δ 7.56 (m, 4H), 7.38 (m, 4H), 7.28 (m, 2H), 2.71 (s, 4H), 1.80 (m, 4H), 1.69 (s, 3H), 1.62 (m, 4H), ppm; ^{13}C NMR ($CDCl_3$) δ 140.0, 128.1, 128.0 126.9, 83.5, 33.3, 23.0 ppm; MS *m/e* 315, 286, 246, 172; HRMS calcd for $C_{23}H_{25}N$ 315.1987, found 315.1989.

Acknowledgment. G.W.G. and F.L.S. thank the donors of the Petroleum Research Fund, administered by the American Chemical Society, for partial support of this research. C.E.S. is grateful to the National Science Foundation (CHE 9215216) for support. C.H.B. is grateful to the University of Vermont Committee on Research and Scholarship for support. J.G.J. is grateful to the University of Vermont College of Arts and Sciences for partial support of this work.

JO952185B

(26) States, D. J.; Haberkorn, R. A.; Ruben, D. J. *J. Magn. Reson.* **1982**, *48*, 286.

(27) Anderson, W. K.; Heider, A. R. *Synth. Commun.* **1986**, *16*, 357.

(28) Weintraub, P. M. *J. Chem. Soc., Chem. Commun.* **1970**, 760.

(29) Fraser, R. R.; Boussard, G.; Postescu, I. D.; Whiting, J. J.; Wigfield, Y. Y. *Can. J. Chem.* **1973**, *51*, 1109.

(30) Bond angles and distances were calculated using the program ORFFE (UCLA Crystallographic package). The torsion angles were calculated using the program MG89 (Trueblood, K.). The sign convention is according to Klyne, W. and Prelog, V. *Experientia* **1960**, 16, 521. Viewing the four-atom A−B−D−E linkage down the B−D bond, the torsion angle is positive if the projection of line B−A must be rotated in a clockwise direction to coincide with the projection of line D−E. The same sign convention is used in the MMX calculations.

(31) The author has deposited atomic coordinates for **BnPh$_2$** with the Cambridge Crystallographic Data Centre. The coordinates can be obtained, on request, from the Director, Cambridge Crystallographic Data Centre, 12 Union Road, Cambridge, CB2 1EZ, UK.